Deforestation Reduces Downwind Precipitation and Soybean Yields in Brazil

Hao Li[1], Corey S. Lesk[2], Deepak K. Ray[3], and Nathaniel D. Mueller[4]

[1]Hydro-Climate Extremes Lab, Ghent University, Ghent, Belgium

[2]Department of Geography, Dartmouth College, Hanover, USA

[3]Institute on the Environment, University of Minnesota, St Paul, USA

[4]Department of Ecosystem Science and Sustainability, Colorado State University, Fort Collins, USA

ABSTRACT

Rapid agricultural expansion has driven unprecedented forest loss worldwide. However, deforestation reduces evaporation locally, potentially triggering precipitation declines in downwind croplands far beyond agricultural frontiers, with consequent impacts on regional crop yields. Using a novel integration of Lagrangian atmospheric moisture tracking and statistical crop modeling, we quantified impacts of evaporation declines on precipitation and soybean yields across Brazilian soybean-producing states during 1982–2015. Our analysis reveals that tree evaporation (i.e., transpiration and canopy interception) contributes roughly one-third of precipitation during the soybean growing season, but recent deforestation has decreased seasonal precipitation by 171 to 326 mm (9–16%). This impact was most pronounced in tropical states near the arc of deforestation in the southern Amazonia, yet the largest reductions in soybean yields (288 kton, or 8% loss) occurred in the southern Brazilian state of Rio Grande do Sul. Cumulatively, deforestation-driven precipitation declines resulted in a total soybean production loss of $\sim$900 kton (3%) in Brazil. These findings demonstrate a self-reinforcing feedback between upwind deforestation and downwind agricultural productivity—revealing a spatial trade-off where agricultural frontier expansion into forests undermines crop yields particularly in established croplands, which in turn may drive demand for additional forest clearing to compensate for these losses. Under continued deforestation and climate change, the feedback loop between forest clearing and agricultural losses is likely to intensify, threatening Brazil's soybean production into the future.

Main Text

Global food security faces unprecedented challenges, requiring a substantial increase in agricultural production by 2050 to meet rising population needs and biofuel consumption[1–3]. This challenge is intensified by increasing climate extremes, such as droughts and heatwaves, during crop growing seasons[4,5]. In response, many countries, particularly in South America, are expanding their agricultural frontiers into natural vegetation regions. As the world's leading soybean producer (∼34% of global production), Brazil has converted over 20 million hectares of forests and savannas into soybean croplands since 2000[6]. However, a growing body of research suggests that this forest cover loss can have profound impacts on regional precipitation patterns, reducing precipitation volumes[7,8], increasing drought frequency[9,10], and delaying rainy season onset[11–13]. Despite these documented precipitation effects, their consequent impacts on agricultural productivity remain largely unquantified at regional scales.

The Amazon rainforest acts as a critical moisture pump, evaporating and recycling vast amounts of water that supports rainfall across key agricultural regions in South America[14]. In particular, Amazonian moisture transport through the South American low-level jet provides 16–25% of annual precipitation over the La Plata river basin[15], where Brazil's southernmost croplands are located. However, as the agricultural frontier expands at the expense of forests, reductions in tree evaporation (i.e., the sum of tree transpiration and canopy interception) have the potential to alter precipitation patterns, far beyond the deforestation regions to the south[16–18]. Agricultural systems critically depend on reliable growing-season rainfall[19–21], particularly as documented in southern Brazil[22], yet quantifying the extent to which changes in tree evaporation propagate through the atmosphere to affect downwind agricultural productivity remains a key research challenge.

To address this gap, we developed an innovative framework combining atmospheric moisture tracking[23] and statistical crop modeling to quantify the cascading impacts of deforestation-driven tree evaporation declines on regional precipitation and agricultural productivity. This framework, demonstrated here using Brazilian soybean production[24], provides a quantitative foundation for understanding forest–precipitation interactions and agricultural implications worldwide. Our findings reveal that agricultural expansion into forests has the potential to create a self-reinforcing feedback in Brazil, where deforestation can reduce regional precipitation and crop yields, potentially enhancing food demand and exacerbating the need for further agricultural expansion[25]. This mechanism likely operates in other major deforestation hotspots for agricultural expansion, such as the Congo Basin and Southeast Asian rainforests, suggesting that maintaining forest cover is crucial for sustaining global agricultural productivity under escalating climate change.

Tree cover and evaporation declines

During the period of 1982–2015, South America experienced unprecedented levels of tree cover loss, with the arc of deforestation (ARC, hatches in Figure 1a)—located between southern Amazonia and the northern Cerrado—emerging as one of Earth's most intensively deforested regions[26]. Using remotely sensed forest cover observations[27], we found that tree cover in this region declined by $\sim$30% during the study period, while deforestation progressively expanded southward into Paraguay and northern Argentina (Figure 1a). Agricultural expansion, primarily driven by global commodity demands, was the primary driver of tree cover loss in South America[28,29]. Consequently, deforestation led to widespread reductions in tree evaporation during the soybean growing season (August–March), with the most significant reductions—exceeding 300 mm—observed in the ARC again (Figure 1b). These declines also persisted across all soybean growth stages (Supplementary Figure S1).

To assess the implications of precipitation changes on soybean yield variability

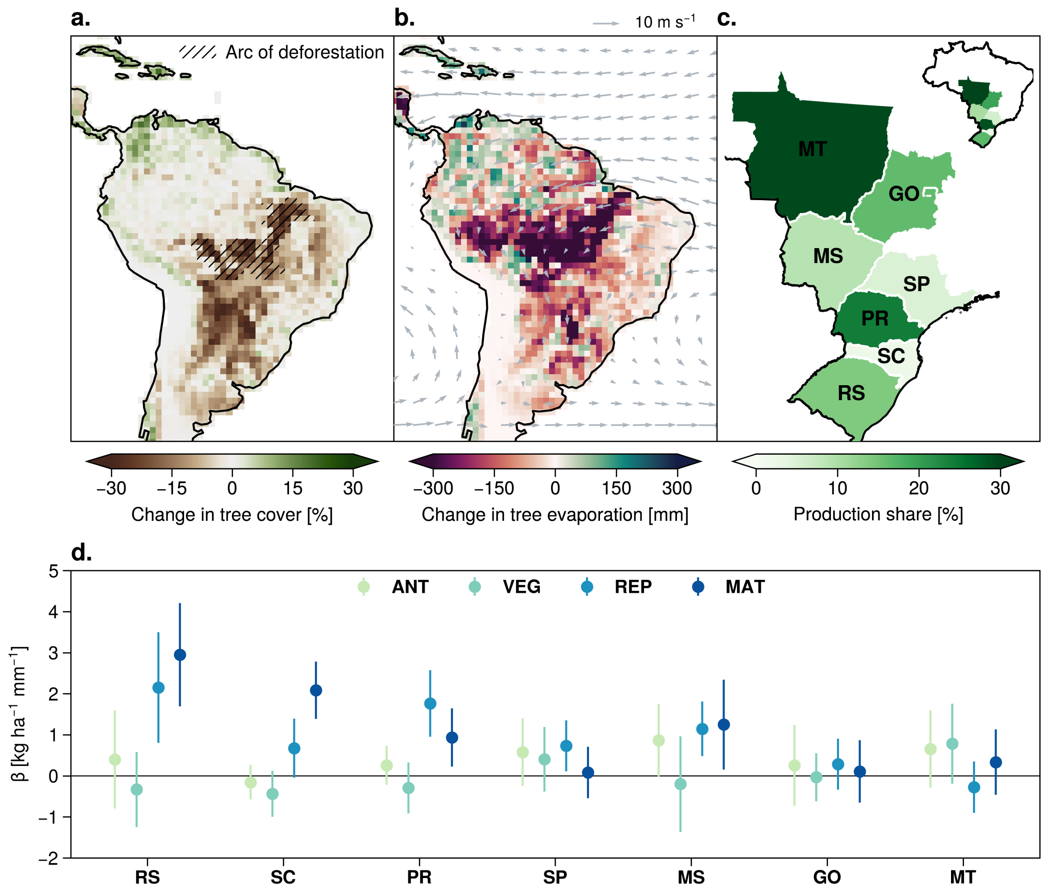

Figure 1. Deforestation, tree evaporation declines, and soybean yield sensitivity to precipitation. a. Change in tree cover fraction (%), calculated as the linear trend multiplied by the study period length (34 years, 1982–2015). The arc of deforestation (ARC) in southern Amazonia is highlighted with black hatches. **b.** Change in tree evaporation (mm) during the soybean growth period (August–March), with arrows indicating prevailing wind direction and magnitude. Growth stage-specific evaporation changes are presented in Supplementary Figure S1. **c.** Share (%) of national soybean production across major soybean-producing states (PR: Paraná, SC: Santa Catarina, RS: Rio Grande do Sul, SP: São Paulo, MS: Mato Grosso do Sul, MT: Mato Grosso, GO: Goiás), calculated by multiplying soybean yield (kg ha^{-1}) by harvested area (ha) in 2000 at 0.5-degree resolution and aggregated to state and country levels. **d.** Sensitivity of soybean yields to precipitation (β, kg ha^{-1} mm^{-1}) during distinct growth stages (ANT: antecedent—August and September, VEG: vegetative—October and November, REP: reproductive—December and January, MAT: maturation—February and March). Points represent mean values with 95% confidence intervals.

across Brazilian soybean states (Figure 1c), we developed a regional-scale statistical crop modelling approach, using the least absolute selection and shrinkage operator (LASSO) regression (see Methods). These models demonstrated strong performance against observations (Supplementary Figure S2 and Supplementary Figure S3). Our results show that, soybean yields in southern Brazilian states—Rio Grande do Sul (RS), Santa Catarina (SC), and Paraná (PR)—exhibited strong sensitivity to precipitation during reproductive and maturation stages, with sensitivity coefficients exceeding 2.0 kg ha^{-1} mm^{-1} during these critical periods (Figure 1d) when atmospheric water demand peaks and reproductive tissues are most vulnerable to drought stress[30,31]. In contrast, tropical soybean yields, particularly in Mato Grosso (MT) and Goiás (GO), showed lower sensitivity to precipitation (Figure 1d) and positive sensitivity to temperature (Supplementary Figure S4), reflecting their energy-limited growth conditions[5,32].

Impacts of tree evaporation changes on precipitation

To identify moisture source regions where precipitation originated from tree evaporation, or in other words, where tree evaporation (E_{tree}) contributed to precipitation (hereafter referred to as $E2P_{tree}$), in Brazil's major soybean-producing states, we employed a Lagrangian-based moisture tracking model integrated with satellite observations (see Methods). Results show, tree evaporation over South America was a major contributor to precipitation across states, where moisture source regions extended from the Amazon through central Brazil into the La Plata basin, with the highest contributions ($>$100 mm) concentrated in southern Amazonia (Figure 2a–d). The contribution varied seasonally: 403 mm (37% of the accumulated precipitation of 1090 mm), increasing to 711 mm (33%) in the vegetative stage, peaking at 949 mm (32%) during reproduction, before declining to 690 mm (27%) in maturation (pie charts in Figure 2a–d). The importance of tree evaporation for precipitation becomes even more crucial at the state level (Figure 2e). MT, bordering Amazonia, exhibited the strongest dependence, receiving 47–265 mm (39–56%) precipitation from tree evaporation across growth stages, but this percent decreased to 64–94 mm (26–37%) in the southernmost state of RS. Moreover, the ARC region alone contributed 17–26% to MT's precipitation (92–110 mm, outlined bars in Figure 2e), highlighting the importance of the deforestation hotspot for agricultural water supply in Brazil.

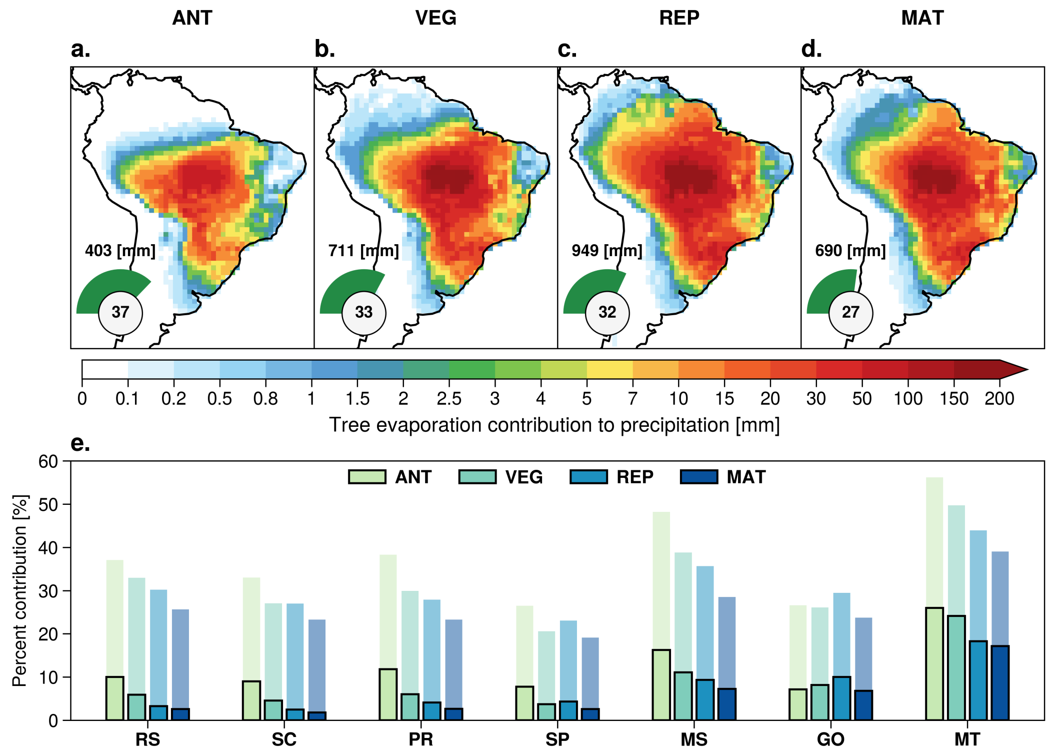

Figure 2. Tree evaporation contribution to precipitation. a–d. Spatial pattern of climatological tree evaporation contributions to precipitation ($E2P_{tree}$, mm) during soybean growth stages: a) antecedent (ANT), b) vegetative (VEG), c) reproductive (REP), and d) maturation (MAT), aggregated across all seven states (state-specific patterns in Supplementary Figure S5). Pie charts show the percentage contribution (%) relative to total precipitation (P), with absolute values (mm) indicated above. **e.** Growth stage-specific tree evaporation contributions (%) across states. Shaded bars represent the percentage of precipitation that originated from tree evaporation across continental South America (relative to total precipitation), while outlined bars show only the portion from the arc of deforestation (ARC). For example, if total precipitation is 500 mm, with 100 mm from South American tree evaporation (including 40 mm from the ARC), the shaded and outlined bars would show 20% and 8%, respectively. Absolute $E2P_{tree}$ values (mm) are provided in Supplementary Figure S6.

We next developed a statistical decomposition method to quantify the impacts of tree evaporation changes under historical deforestation on precipitation (see Methods). Our results showed that tree evaporation declines substantially reduced precipitation over soybean regions, with the most pronounced impacts—exceeding 70 mm declines—observed within the ARC (Figure 3a–d). These reductions followed similar seasonal variability, with -171 mm (16% of accumulated precipitation) during the antecedent period, -229 mm (11%) in the vegetative stage, -326 mm (11%) during reproduction, and -226 mm (9%) during maturation. The magnitude of these impacts also varied significantly across states (shaded bars in Figure 3e), with MT experiencing the largest reductions up to 107 mm ($\sim$18%) during reproduction, and the effects declining southward (20–41 mm, 7–16%). Importantly, tree evaporation changes within the ARC accounted for more than half of the precipitation decline in tropical states (outlined bars in Figure 3e). The magnitude and consistency of these deforestation-induced precipitation declines suggest that their impacts on agricultural productivity are likely to be widespread.

Estimated reductions in soybean yields under deforestation

We next examined how widespread tree evaporation declines affected soybean yields in Brazil, by combining the yield sensitivity to precipitation (Figure 1d) with absolute precipitation reductions driven by tree evaporation changes (Supplementary Figure S9). In tropical states, although yield sensitivity to precipitation was relatively lower, substantial precipitation reductions led to a considerable yield loss (Figure 4a). For instance, in Mato Grosso do Sul (MS), tree evaporation declines resulted in a total yield loss of 119 kg ha^{-1} during the growing season. In contrast, southern states, despite experiencing smaller precipitation reductions, suffered greater losses due to their higher yield sensitivity. For example, RS lost 125 kg ha^{-1} in total, with the most severe reductions occurring during the critical reproductive (46 kg ha^{-1} losses) and maturation phases (63 kg ha^{-1} losses).

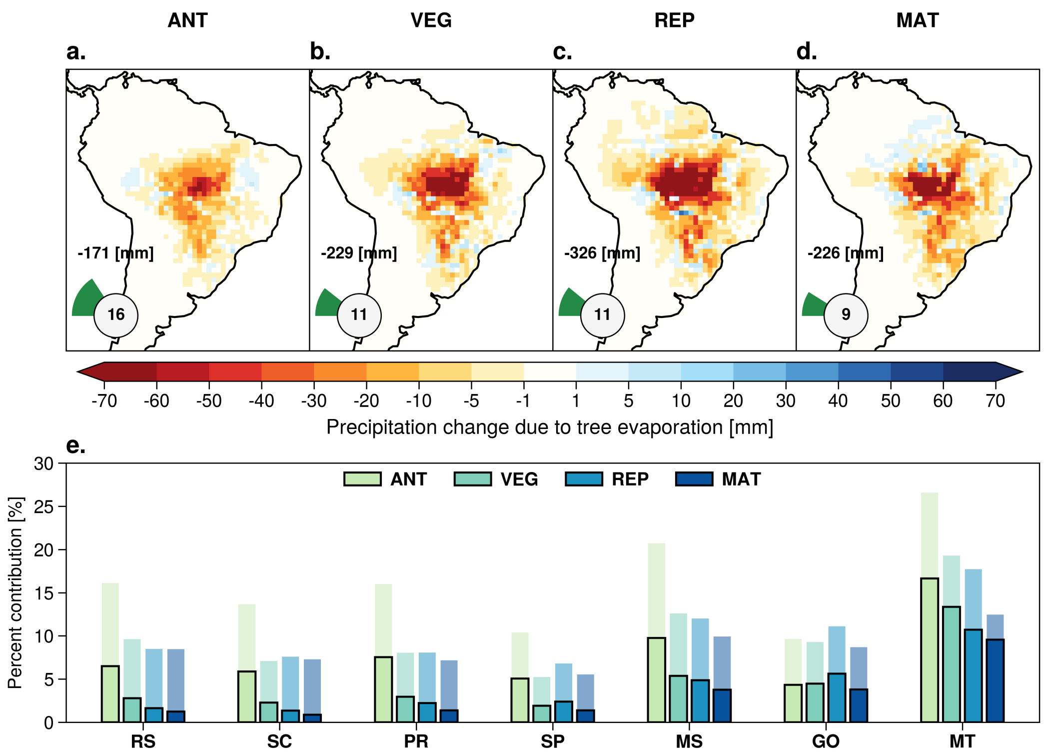

Figure 3. Precipitation reductions caused by tree evaporation declines. a–d. Spatial patterns of precipitation changes (mm) caused by tree evaporation during soybean growth stages: a) antecedent (ANT), b) vegetative (VEG), c) reproductive (REP), and d) maturation (MAT), aggregated across all seven Brazilian states (state-specific patterns in Supplementary Figure S8). Pie charts show these reductions as percentages of total precipitation (P), with absolute values (mm) indicated above. **e.** Growth stage-specific precipitation reductions (%) across states during 1982–2015. Shaded bars represent the percentage reduction in precipitation (relative to total precipitation) caused by tree evaporation across continental South America, while outlined bars show only the portion from the arc of deforestation (ARC). For example, in a region receiving 500 mm total precipitation, if tree evaporation decline causes a 60 mm reduction (including 40 mm from the ARC), the shaded and outlined bars would show -12% and -8%, respectively. Absolute reduction values are provided in Supplementary Figure S9.

We further scaled these yield impacts to estimate total production losses using soybean harvested areas circa 2000[33] as the reference baseline. The yield reductions translated to substantial production losses totaling 923 kton across all studied states (Figure 4b). RS experienced the largest absolute decline (288 kton, 8% of regional production), followed by MT (243 kton, 3%), PR (194 kton, 3%), and MS (124 kton, 5%). Based on average soybean prices during 2000–2015 ($\sim$400 per ton), these losses amounted to approximately 369 million dollars, demonstrating that deforestation creates hidden economic costs extending far beyond the deforestation frontier. Given substantial expansion of soybean cultivation after 2000[6], these estimates are probably conservative.

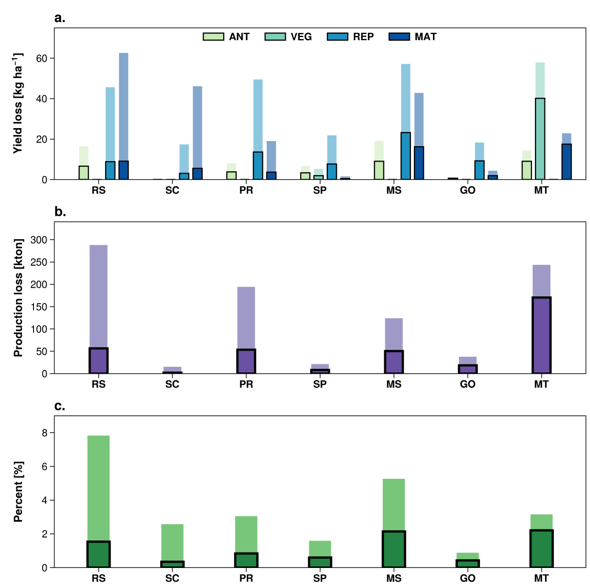

Figure 4. Soybean productivity losses due to tree evaporation-driven precipitation declines. a. Estimated soybean yield reductions (kg ha^{-1}) during growth stages, calculated by multiplying precipitation sensitivity (Figure 1d) by precipitation decreases caused by tree evaporation (Supplementary Figure S9). **b.** Absolute soybean production declines (kton), calculated as the product of total yield declines across stages and harvest area circa 2000. **c.** Percent of production declines relative to total production across states. Shaded bars represent impacts from tree evaporation declines across continental South America, while outlined bars show the portion specifically from the arc of deforestation (ARC).

Self-reinforcing feedback of agricultural expansion

Our analysis reveals that forest clearing for agricultural expansion undermines soybean productivity at larger spatial scales through atmospheric moisture recycling and transport. Across Brazil, deforestation-induced evaporation declines substantially reduce precipitation (9–16%) in agricultural regions, resulting in a total soybean production loss of 923 kton (approximately 3% of national output), with impacts extending far beyond deforestation frontiers.

These yield reductions exhibited considerable spatial variability across Brazil. While direct precipitation reductions were most apparent in the immediate regions that are closest to the deforestation front (Figure 3e), the largest deforestation-induced reductions in soybean yield occurred in drier regions (Figure 4), where strong moisture limitations have increased the sensitivity of crops to water availability[30,31]. This heightened sensitivity produced some of the most severe implications in southern Brazil's agricultural heartland, where even moderate precipitation reductions led to significant yield losses. Such vulnerability is particularly pronounced because these southern regions operate closer to critical water thresholds for optimal soybean development, particularly during reproductive stages (Figure 3e) when water stress most severely impacts pod formation and filling.

The study specifically focuses on how deforestation-driven evaporation declines affect precipitation and agricultural productivity. While deforestation also influences atmospheric (thermo)dynamics particularly in the small scale[17,34], previous research at comparable regional scales demonstrates that evaporation changes serve as the dominant driver of precipitation patterns in these contexts[7,16,18], supporting our methodological emphasis on evaporation impacts on precipitation and soybean in Brazil.

Consequently, these findings demonstrate that expansion into forests is directly limiting the capacity for soybean production across broad spatial scales. While current deforestation-induced yield reduction ($\sim$3%) may be temporarily offset by newly cleared agricultural land, this balance is inherently unsustainable and increasingly precarious[25]. As deforestation continues alongside climate change[35,36], these hydrological impacts will likely intensify non-linearly[37], progressively constraining regional agricultural productivity. Declining soybean productivity may further drive additional demand for cropland expansion, triggering a self-reinforcing feedback loop that has the potential to accelerate over the coming decades. This positive feedback operates as agricultural forest clearing continues, causing precipitation reductions that lower soybean yields, which in turn enhances the demand for further deforestation.

In conclusion, our findings reveal that forest cover loss significantly reduces downwind precipitation and soybean productivity far beyond deforestation regions. Therefore, maintaining forest cover is not merely an environmental concern but also an economic and political imperative for ensuring long-term agricultural outputs and food security[38]. The self-reinforcing feedback loop between forest clearing and agricultural losses demonstrated here calls for integrated forest-agricultural management policies that recognize the connection between forest conservation and sustained agricultural productivity. Future agricultural planning must carefully consider the trade-offs between short-term expansion gains and the long-term productivity losses that result from disrupting critical hydrological cycles[17,25].

Methods

Soybean states and growth stages

Our study focused on Brazil's seven major soybean-producing states, which account for approximately 90% of national production (Figure 1c). The southern states–Rio Grande do Sul (RS), Santa Catarina (SC), and Paraná (PR)—have a subtropical climate where soybean yields are highly sensitive to precipitation variability. In contrast, the central and tropical states—São Paulo (SP), Mato Grosso do Sul (MS), Goiás (GO) and Mato Grosso (MT)—experience a seasonal wet-dry climate (Supplementary Figure S11), where agriculture is generally energy-limited during the soybean growing season. MT, Brazil's leading soybean producer, accounts for one-third of national output and intersects with the arc of deforestation (Figure 1a), a region experiencing substantial tree cover loss between 1982 and 2015. PR and RS contribute 13% and 11% of national production, respectively (Figure 1c).

We analyzed soybean yield response to precipitation across four critical growth stages: the antecedent period (ANT, August–September) for establishing baseline soil moisture conditions; the vegetative stage (VEG, October–November) characterized by emergence and leaf development; the reproductive phase (REP, December–January) encompassing flowering and pod formation; and the maturation stage (MAT, February–March) focusing on pod filling and yield determination. While growing season lengths vary across regions, this standardized framework enabled systematic cross-regional comparison while capturing essential phenological stages. For temporal consistency, we referenced soybean growth years by their harvest year (e.g., 2001 refers to October 2000 to March 2001). Cropland extent was based on a gridded dataset circa 2000[33]. The arc of deforestation in the south of Amazonia (ARC) is identified in this study when tree cover[27] loss exceeds 10% over 0.5-degree grids during the study period.

Quantifying yield response to precipitation

Here, we developed the following state-specific linear regression models to predict soybean yields:

$$Y = \sum_{s=1}^{s=4} (\beta_{P_s} \times P_s) + \beta_{T_g} \times T_g + \beta_{year} \times year + \beta_{year^2} \times year^2 \quad (1)$$

where Y represents soybean yield (kg ha^{-1}), P_s is precipitation (mm) during four growth stages: ANT ($s = 1$), VEG ($s = 2$), REP ($s = 3$), and MAT ($s = 4$), and T_g is the average growing-season (daily mean) air temperature (°C). The time term ($year$ and $year^2$) accounts for technological advancements in agronomic practices over time, such as improved cultivars, fertilization, and management techniques. We used growth-stage-aggregated rather than monthly precipitation to avoid overfitting while capturing the sensitivity of soybean yields to water availability. We also tested more complex formulations (including quadratic temperature terms and precipitation–temperature interactions) but adopted this simpler model structure as the alternatives showed minimal R^2 improvements while introducing potential overfitting issues. This model also allows us to more directly quantify the effects of precipitation changes on soybean yields—a critical consideration for assessing deforestation impacts on agricultural productivity through atmospheric moisture recycling.

We implemented the Least Absolute Shrinkage and Selection Operator (LASSO) regression to optimize model performance through variable selection and regularization. Model uncertainty was quantified using 1000 bootstrap iterations, with each iteration randomly allocating 2/3 of the responses-predictor pairs for calibration, and the remaining 1/3 for validation. Model performance was assessed through determination of coefficients (R^2) between observed and predicted yields for both calibration and validation datasets. The iterations also provided distributions of regression coefficients (β) and R^2, allowing calculation of their confidence intervals (CIs). Our model exhibits strong performance, achieving the high determination coefficients in both train and test data (mean $R^2 > 0.80$ and 0.60, Supplementary Figure S2), and accurately predicting historical soybean yields ($R^2 > 0.70$ across states, Supplementary Figure S3).

Soybean yield statistics were obtained from Brazil's national agricultural database Instituto Brasileiro de Geografia e Estatística[24]. For climate variables, we used precipitation data from the Multi-Source Weighted-Ensemble Precipitation (MSWEP) at 0.1° spatial resolution[39], and 2-m air temperature data from the European Center for Medium-Range Weather Forecasts ReAnalysis (ERA) 5 at 0.25° spatial resolution[40].

We calculated cropland area-weighted precipitation totals for each state across four growth stages, while temperature was averaged over the entire soybean growth period (August–March) to capture thermal conditions throughout crop development.

Atmospheric moisture tracking framework

In this study, we employed the Lagrangian particle dispersion model FLEXPART version 10.4[23] driven with reanalysis at 1° resolution to track air parcels through the atmosphere. The model was initialized with approximately 3 million air parcels (each with mass 1.697x10^{12} kg) distributed homogeneously across the globe. Each air parcel carries properties including specific humidity, potential temperature and density, with FLEXPART tracking their three-dimensional positions and properties over time. The outputs provided information on parcel positions (longitude, latitude, height), properties (density, specific humidity), and boundary layer characteristics, enabling the following construction of source-sink relationship of precipitation[41]. While the simulations incorporated both 6-hourly reanalysis and 3-hourly forecasts to improve trajectory accuracy through better representation of turbulence, our source-sink relationship analysis of precipitation used only 6-hourly reanalysis outputs.

Next, we constructed the source-sink relationship of precipitation based on the trajectories tracked, through three steps: (1) diagnosis, (2) attribution, and (3) bias correction[42]. The diagnosis step evaluates all air parcels at consecutive 6-hourly time steps, quantifying precipitation and evaporation to establish detection metrics. During the step of attribution, we selected air parcels over target regions (that is, Brazilian soybean states under study, Figure 1c) and then tracked their backward trajectories. This identifies the evaporation and precipitation events through specific detection criteria: evaporation occurs when the change of specific humidity is higher to 0 g kg^{-1} in a 6-hourly time interval, and precipitation events are identified when relative humidity exceeds 80%[42,43]. In the third step, the framework conducts bias correction using observational datasets: MSWEP for precipitation and GLEAM over land[44] and OAFlux over ocean[45] for surface evaporation. Furthermore, using daily tree evaporation (that is, the sum of tree transpiration and interception loss) fraction (relative to total evaporation), we identified moisture source regions where tree evaporation contributes to precipitation, or precipitation originates from tree evaporation[46,47].

We quantified tree evaporation contributions to precipitation ($E2P_{tree}$) across soybean growth stages at both state and continental scales. At the state level, we calculated the relative contribution of each source region (Figure 2e) by comparing absolute $E2P_{tree}$ values (Supplementary Figure S6) to total precipitation received by individual states (Supplementary Figure S11). For continental-scale patterns, we aggregated moisture sources across all seven study states while preserving the spatial identity of source regions (Supplementary Figure S5). We then evaluated the relative importance of these contributions by comparing them to the total precipitation received by all states combined, conducting separate analyses for each growth stage (Figure 2a–d).

Uncovering tree evaporation impacts on precipitation

Since precipitation is inherently a fraction of evaporation, we express $E2P_{tree}$ as the product of tree evaporation (E_{tree}) and a parameter (λ) that represents the transport and conversion efficiency of evaporated moisture to precipitation:

$$E2P_{tree} = \lambda \times E \tag{2}$$

To analyze long-term changes in $E2P_{tree}$, we used a linearization approach that assumes independence between E_{tree} and λ at climatological timescales (>30 years). This assumption enables us to express temporal changes in $E2P_{tree}$ by differentiating

Equation 2 with respect to time:

$$\frac{\partial E2P_{tree}}{\partial t} = \frac{\partial E_{tree}}{\partial t} \times \lambda \ + \frac{\partial \lambda}{\partial t} \times E_{tree} \tag{3}$$

Taking time averages, Equation 3 can be rewritten as follows:

$$S_{E2P_{tree}} = S_{E_{tree}} \times \bar{\lambda} + S_{\lambda} \times \bar{E_{tree}} + \delta \tag{4}$$

where S represents the slope of the linear regression (trend) for $E2P_{tree}$, E_{tree} and λ, respectively, with bars denoting climatological averages and δ being the residual of the approximation. The term $S_{E_{tree}} \times \bar{\lambda}$ specifically quantifies the impact of E_{tree} changes on precipitation.

Note that, the transformation from Equation 3 to 4 involves two simplifications suited to our climatological analysis: we approximate the temporal derivatives using linear regression slopes (e.g., $\frac{\partial E_{tree}}{\partial t}$ as $S_{E_{tree}}$), and decompose time-averaged products into products of averages (denoted by bars). However, the robustness of these approximations is empirically validated in Supplementary Figure S10, which shows that residual terms account for less than 1% of the total $E2P_{tree}$ changes (Supplementary Figure S7). This also confirm that nonlinear interactions between E_{tree} and λ changes play a minor role at the climatological scale.

Similarly, we quantified the impact of tree evaporation declines on precipitation at both state and continental scales. For individual states (Figure 3e), we calculated precipitation reductions (i.e., $S_{E_{tree}} \times \bar{\lambda}$, Supplementary Figure S9) relative to seasonal totals (Supplementary Figure S11). At the continental scale (Figure 3a–d), we aggregated these changes across all study states (Supplementary Figure S8), with analyses conducted separately for each soybean growth stage.

Quantifying tree evaporation impacts on soybean yields

To quantify how tree evaporation changes affect soybean productivity, we combined crop-climate sensitivity analysis with precipitation changes driven by tree evaporation declines. We estimated soybean yield sensitivity to precipitation (β, kg ha^{-1} mm^{-1}) across growth stages using LASSO regression (see above and Figure 1d), and then quantified how historical tree evaporation declines altered precipitation patterns (Supplementary Figure S9). For each growth stage, yield impacts were calculated by combining precipitation reductions with corresponding yield sensitivities. For example, with a yield sensitivity of 2 kg ha^{-1} mm^{-1} to precipitation, a 10 mm reduction in precipitation due to decreased tree evaporation would result in a yield loss of 20 kg ha^{-1}. We included only positive sensitivities exceeding 0.10 kg ha^{-1} mm^{-1}, as weak or negative responses typically indicate energy-limited conditions where increased precipitation reduces solar radiation[5,48]. Total state-level production losses were estimated by multiplying yield reductions with harvested areas circa 2000[33].

Data availability

Soybean yield statistics were obtained from https://www.ibge.gov.br. The harvest area is available from https://www.dante-project.org/datasets/mirca2K. MEaSUREs Vegetation Continuous Fields is acquired from https://lpdaac.usgs.gov/products/vcf5kyrv001. GLEAM data are available through https://www.gleam.eu. OAFlux data can be retrieved from https://oaflux.whoi.edu/data-access. ERA data were accessed from https://cds.climate.copernicus.eu/cdsapp#!/dataset. MSWEP data are available through http://www.gloh2o.org.

Code availability

The FLEXPART model can be downloaded via https://www.flexpart.eu. The version of the moisture tracking framework used for analysis of FLEXPART data is preserved at https://doi.org/10.5281/zenodo.5788506. Python scripts for the analysis are available upon request from Dr. Hao Li.

Acknowledgements

The computational resources and services used in this work were provided by the VSC (Flemish Supercomputer Center), funded by the FWO and the Flemish Government, Department of Economy, Science and Innovation (EWI). H.L. thanks the China Scholarship Council (CSC) for financial support under grant agreement 202006350051. H.L. is grateful to Prof. Diego G. Miralles and Dr. Damián Insua-Costa for valuable discussions during early stages of this work. H.L. thanks Dr. Thomas W. Crowther for constructive suggestions on this manuscript.

Author contributions

H.L. conceived the study, designed the experiments, and conducted the analysis. H.L., and C.L., contributed to data analysis and interpretation. All authors contributed to writing the original draft and participated in several rounds of revisions.

Competing interests

The authors declare no competing interests.

References

1. Van Dijk, M., Morley, T., Rau, M. L. & Saghai, Y. A meta-analysis of projected global food demand and population at risk of hunger for the period 2010–2050. *Nat. Food* **2**, 494–501 (2021).

2. Tilman, D., Balzer, C., Hill, J. & Befort, B. L. Global food demand and the sustainable intensification of agriculture. *Proc. national academy sciences* **108**, 20260–20264 (2011).

3. Hunter, M. C., Smith, R. G., Schipanski, M. E., Atwood, L. W. & Mortensen, D. A. Agriculture in 2050: recalibrating targets for sustainable intensification. *Bioscience* **67**, 386–391 (2017).

4. Lesk, C. *et al.* Compound heat and moisture extreme impacts on global crop yields under climate change. *Nat. Rev. Earth & Environ.* **3**, 872–889 (2022).

5. Li, H. *et al.* Land–atmosphere feedbacks contribute to crop failure in global rainfed breadbaskets. *npj Clim. Atmospheric Sci.* **6**, 51 (2023).

6. Song, X.-P. *et al.* Massive soybean expansion in South America since 2000 and implications for conservation. *Nat. sustainability* **4**, 784–792 (2021).

7. Smith, C., Baker, J. & Spracklen, D. Tropical deforestation causes large reductions in observed precipitation. *Nature* **615**, 270–275 (2023).

8. Spracklen, D. & Garcia-Carreras, L. The impact of Amazonian deforestation on Amazon basin rainfall. *Geophys. Res. Lett.* **42**, 9546–9552 (2015).

9. Jiang, Y. *et al.* Modeled response of south american climate to three decades of deforestation. *J. Clim.* **34**, 2189–2203 (2021).

10. da Silva, S. S. *et al.* Amazon climate extremes: Increasing droughts and floods in brazil's state of acre. *Perspectives Ecol. Conserv.* **21**, 311–317 (2023).

11. Leite-Filho, A. T., de Sousa Pontes, V. Y. & Costa, M. H. Effects of deforestation on the onset of the rainy season and the duration of dry spells in southern Amazonia. *J. Geophys. Res. Atmospheres* **124**, 5268–5281 (2019).

12. Fu, R. *et al.* Increased dry-season length over southern Amazonia in recent decades and its implication for future climate projection. *Proc. Natl. Acad. Sci.* **110**, 18110–18115 (2013).

13. Butt, N., De Oliveira, P. A. & Costa, M. H. Evidence that deforestation affects the onset of the rainy season in rondonia, brazil. *J. Geophys. Res. Atmospheres* **116** (2011).

14. Flores, B. M. *et al.* Critical transitions in the Amazon forest system. *Nature* **626**, 555–564 (2024).

15. Chug, D., Dominguez, F. & Yang, Z. The Amazon and La Plata River Basins as Moisture Sources of South America: Climatology and Intraseasonal Variability. *J. Geophys. Res. Atmospheres* **127**, e2021JD035455 (2022).

16. Khanna, J., Medvigy, D., Fueglistaler, S. & Walko, R. Regional dry-season climate changes due to three decades of Amazonian deforestation. *Nat. Clim. Chang.* **7**, 200–204 (2017).

17. Lawrence, D. & Vandecar, K. Effects of tropical deforestation on climate and agriculture. *Nat. climate change* **5**, 27–36 (2015).

18. Staal, A. *et al.* Forest-rainfall cascades buffer against drought across the Amazon. *Nat. Clim. Chang.* **8**, 539–543 (2018).

19. Ray, D. K., Gerber, J. S., MacDonald, G. K. & West, P. C. Climate variation explains a third of global crop yield variability. *Nat. communications* **6**, 5989 (2015).

20. Lobell, D. B., Schlenker, W. & Costa-Roberts, J. Climate trends and global crop production since 1980. *Science* **333**, 616–620 (2011).

21. Li, H., Keune, J., Gou, Q., Holgate, C. M. & Miralles, D. Heat and moisture anomalies during crop failure events in the southeastern australian wheat belt. *Earth's Futur.* **12**, e2023EF003901 (2024).

22. Zanon, A. J., Streck, N. A. & Grassini, P. Climate and management factors influence soybean yield potential in a subtropical environment. *Agron. J.* **108**, 1447–1454 (2016).

23. Pisso, I. *et al.* The Lagrangian particle dispersion model FLEXPART version 10.4. *Geosci. Model. Dev.* **12**, 4955–4997 (2019).

24. of Geography, B. I. & Statistics. Municipal agricultural production: Brazil's agricultural municipal production survey. Statistical Report (2023). Accessed: 2023.

25. Oliveira, L. J., Costa, M. H., Soares-Filho, B. S. & Coe, M. T. Large-scale expansion of agriculture in amazonia may be a no-win scenario. *Environ. Res. Lett.* **8**, 024021 (2013).

26. Ometto, J. P., Aguiar, A. P. D. & Martinelli, L. A. Amazon deforestation in brazil: effects, drivers and challenges. *Carbon Manag.* **2**, 575–585 (2011).

27. Hansen, M. & Song, X.-P. Vegetation continuous fields (vcf) yearly global 0.05 deg (2018).

28. Curtis, P. G., Slay, C. M., Harris, N. L., Tyukavina, A. & Hansen, M. C. Classifying drivers of global forest loss. *Science* **361**, 1108–1111 (2018).

29. Pendrill, F. *et al.* Disentangling the numbers behind agriculture-driven tropical deforestation. *Science* **377**, eabm9267 (2022).

30. Battisti, R., Sentelhas, P. C. & Boote, K. J. Inter-comparison of performance of soybean crop simulation models and their ensemble in southern brazil. *Field Crop. Res.* **200**, 28–37 (2017).

31. Fiorini, A. C. O. *et al.* How climate change is impacting the brazilian agricultural sector: evidence from a systematic literature review. *Environ. Res. Lett.* **19**, 083001 (2024).

32. Lesk, C. *et al.* Stronger temperature–moisture couplings exacerbate the impact of climate warming on global crop yields. *Nat. food* **2**, 683–691 (2021).

33. Portmann, F. T., Siebert, S. & Döll, P. MIRCA2000—Global monthly irrigated and rainfed crop areas around the year 2000: A new high-resolution data set for agricultural and hydrological modeling. *Glob. biogeochemical cycles* **24** (2010).

34. Eiras-Barca, J. *et al.* Changes in South American hydroclimate under projected Amazonian deforestation. *Annals New York Acad. Sci.* **1472**, 104–122 (2020).

35. Rochedo, P. R. *et al.* The threat of political bargaining to climate mitigation in brazil. *Nat. climate change* **8**, 695–698 (2018).

36. Rezaei, E. E. *et al.* Climate change impacts on crop yields. *nature reviews earth & environment* **4**, 831–846 (2023).

37. Bonan, G. B. Forests and climate change: forcings, feedbacks, and the climate benefits of forests. *science* **320**, 1444–1449 (2008).

38. Costanza, R. *et al.* Changes in the global value of ecosystem services. *Glob. environmental change* **26**, 152–158 (2014).

39. Beck, H. E. *et al.* MSWEP: 3-hourly 0.25 global gridded precipitation (1979–2015) by merging gauge, satellite, and reanalysis data. *Hydrol. Earth Syst. Sci.* **21**, 589–615 (2017).

40. Soci, C. *et al.* The era5 global reanalysis from 1940 to 2022. *Q. J. Royal Meteorol. Soc.* **150**, 4014–4048 (2024).

41. Stohl, A., Forster, C., Frank, A., Seibert, P. & Wotawa, G. The lagrangian particle dispersion model flexpart version 6.2. *Atmospheric Chem. Phys.* **5**, 2461–2474 (2005).

42. Keune, J., Schumacher, D. L. & Miralles, D. G. A unified framework to estimate the origins of atmospheric moisture and heat using lagrangian models. *Geosci. Model. Dev.* **15**, 1875–1898 (2022).

43. Sodemann, H., Schwierz, C. & Wernli, H. Interannual variability of Greenland winter precipitation sources: Lagrangian moisture diagnostic and North Atlantic Oscillation influence. *J. Geophys. Res. Atmospheres* **113** (2008).

44. Martens, B. *et al.* GLEAM v3: Satellite-based land evaporation and root-zone soil moisture. *Geosci. Model. Dev.* **10**, 1903–1925 (2017).

45. Yu, L. & Weller, R. Objectively analyzed air-sea heat fluxes (oaflux) for the global oceans. *Bull. Am. Met. Soc* **88**, 527–539 (2007).

46. Te Wierik, S. *et al.* The contribution of transpiration to precipitation over african watersheds. *Water Resour. Res.* **58**, e2021WR031721 (2022).

47. Te Wierik, S. *et al.* Critical importance of tree and non-tree vegetation for african precipitation. *Geophys. Res. Lett.* **51**, e2023GL103274 (2024).

48. Rigden, A., Mueller, N., Holbrook, N., Pillai, N. & Huybers, P. Combined influence of soil moisture and atmospheric evaporative demand is important for accurately predicting us maize yields. *Nat. Food* **1**, 127–133 (2020).